

Length and diameter determination of rod-like particles using Depolarized Dynamic Light Scattering (DDLS)

Key Words: *Dynamic Light Scattering, particles size measurement, injectable, syringe, protein, contactless measurement, Vasco Kin.*

Contact@cordouan-tech.com

Anisotropic nanoparticles (NP), such as nanorods, nanotubes, nanodiscs etc. are widely used in such fields as medicine (fluorescent enhancers, tumor markers and light receptors), electronics (molecular electronic devices, sources of local heating) and many others^[1]. Self-assemblies of these NPs are also used for fabrication of advanced materials^[2] in which shape and size of anisotropic NPs highly affect their properties and, as a result, have an influence on their efficiency in the final application. Consequently, knowledge of NP geometrical dimensions (length, diameter and aspect ratio) at different stages of their synthesis and application is critical.

Nowadays, Transmission Electron Microscopy (TEM) is one of the common direct techniques used for studying NP shape and dimensions characteristics. However, such a method involves complex sample preparation steps as well as long observation time which prevent from using it as a routine characterization technique. Since observation is achieved on a limited number of particles deposited on the TEM grid, the representativeness of sizes and shapes distributions evaluation is also statistically questionable. In such cases, indirect optical methods like Dynamic Light Scattering (DLS) measurement can circumvent these limitations with some key benefits: limited sample preparation (measurement directly in liquid suspensions), ease of use, short measurement time (data acquisition and processing in less than a minute), strong statistical representativeness of the results (the scattered light beams probing trillions of NPs at once), etc.

However, standard DLS analysis assumes that particles are spherical and thus can only provide information on an average hydrodynamic diameter i.e. the effective diameter of a sphere having the same translational coefficient than the NPs; In the case of anisotropic nanoparticles, one can use a refined version of DLS named Depolarized Dynamic Light Scattering (DDLS), which allows size and shape characterization of very small particles (down to few nanometers).^[3]

In this communication, we demonstrate the measurement capabilities of a new and patented commercial DDLS system developed by Cordouan technologies (named Thetis)^[4] by presenting experimental results on small gold nanorods. The DDLS results are compared with TEM ones to qualify the precision of the measurements by this method.

DDLS Principle:

Standard DLS system allows determining NP diameter through the measurement of their diffusion behavior (Brownian motion) by monitoring – at a given observation angle – the fluctuations of the light scattered by the NP suspensions. More precisely, the Auto Correlation Function (ACF) calculated from the light intensity fluctuations gives access to a translational diffusion coefficient (D_t) which is related to the hydrodynamic radius¹ of the particle by the well-known Stokes- Einstein equation ^[5,6]. In the case of anisotropic particles, their dynamics in the liquid is strongly affected by their size and shape and comprises both translational and rotational random motions, respectively described by a translation diffusion coefficient (D_t) and a rotational diffusion coefficient (D_r). Using the properties of linearly polarized light it becomes possible to measure D_t and D_r to deduce the size and aspect ratio of the anisotropic particles. ^[7]

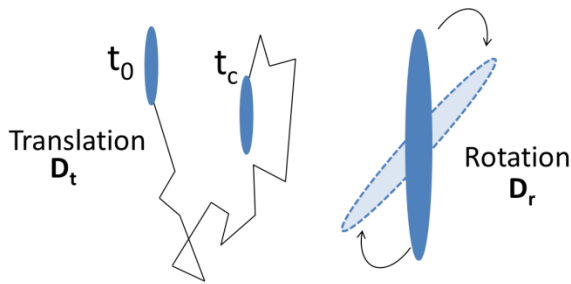
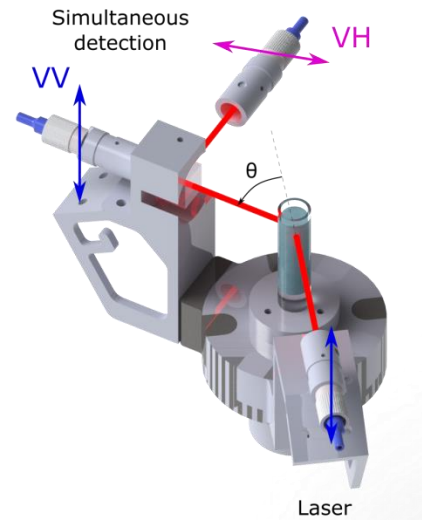


Figure1. Illustration of the Brownian motion of anisotropic particles where translational diffusion coefficient (D_t) and rotational diffusion coefficient (D_r) are its main characteristics.

Figure 2 illustrates the optical setup of the Thetis® DDLS instrument from Cordouan Technologies. First, a vertically polarized incident laser beam is focused onto the sample. Scattered light is then collected at different angles (θ) using a compact motorized goniometer. Use of high quality (Glan-Thomson) biprism enables splitting the scattered beam toward two distinct detection channels according to the light polarization, allowing the measurement of the vertically polarized (v-v) and the horizontally depolarized (v-h) scattered light separately with a very low optical cross-talk (<-35dB) between the two polarization channels.



In the case of anisotropic particles, the v-v and v-h detection channels lead to two different ACFs calculated from the corresponding scattered intensity fluctuations, respectively $G_w(\tau)$ and $G_{vh}(\tau)$ given by equation 1 and 2 below:

Figure 2. Scheme of the DDLS instrument optical setup.

$$G_{VV}(\tau) = A_1 \exp^{-(\Gamma_t + \Gamma_r)\tau} + A_2 \exp^{-(\Gamma_t)\tau} + B \tag{eq.1}$$

$$G_{VH}(\tau) = A_3 \exp^{-(\Gamma_t + \Gamma_r)\tau} + B' \tag{eq.2}$$

¹ i.e. the radius of a homogeneous sphere having the same mobility than the considered particles

where τ is the delay time of ACF, A_1 , A_2 and A_3 are weighting factors and B and B' are background constants.

One can notice that both ACFs contain a “mixed mode” combining the translational decay rate Γ_t and the rotational decay rate Γ_r . These decay rates are related to their corresponding diffusion coefficients by the following equations:

$$\Gamma_t = D_t q^2 \tag{eq.3}$$

$$\Gamma_r = 6D_r \tag{eq.4}$$

Where q is the scattering wave vector defined by $q = \frac{4\pi n}{\lambda} \sin(\theta/2)$ with n the suspension refractive index, λ the laser wavelength, and ϑ the detection angle.

Thus, one method to determine D_t and D_r from DDLS measurements consists in plotting the mixed mode ($\Gamma_t + \Gamma_r$), obtained either from G_{vh} or either from the fast G_{vv} relaxation, as a function of q^2 . The linear regression calculated from these data should then have a slope equal to D_t and its extrapolation at $q = 0$ equal to $6D_r$ (see fig.3). One can note that D_t can also be determined by plotting the pure translational mode obtained from the slow G_{vv} relaxation.

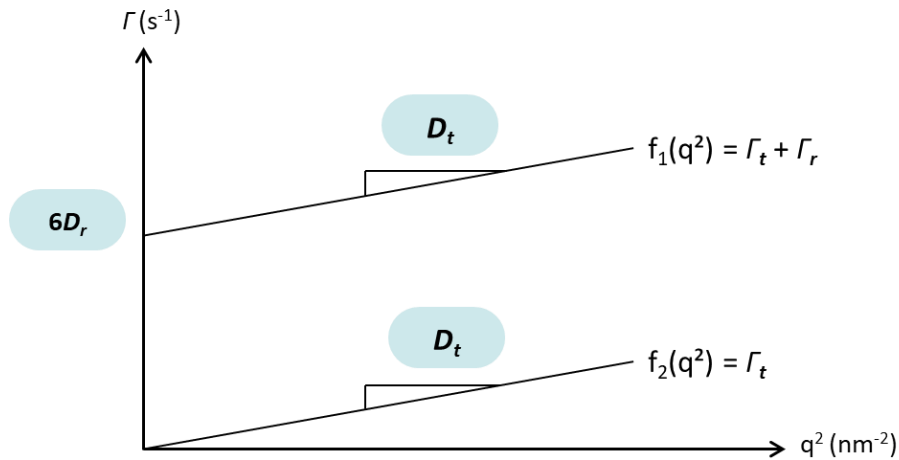


Figure 3: Graphical determination of the translational and rotational diffusion constants from the decay rates determined by fitting the autocorrelation functions $G_{vv}(\tau)$ and $G_{vh}(\tau)$ of scattered light intensity fluctuations in parallel (v-v) and in perpendicular (v-h) polarizations.

The determination of two different diffusion coefficients allows calculating two dimensions of anisotropic particles, typically the length L and the aspect ratio L/w (where w is the width of particles which in case of cylinders is their diameter. The width is calculated from obtained L and L/w). Various hydrodynamic models can be used in such calculations depending on the targeted shape of particles. For

example, in the case of straight cylinders, D_t and D_r can be determined using general equations 5 and 6 [7].

$$D_r = \frac{3k_B T}{\pi \eta L^3} f\left(\frac{L}{w}\right) \tag{eq.5}$$

$$D_t = \frac{k_B T}{3\pi \eta L} f\left(\frac{L}{w}\right) \tag{eq.6}$$

Where T is the temperature, k_B is the Boltzmann constant, η the dynamic viscosity of the continuous phase and $f\left(\frac{L}{w}\right)$ is a model-dependent function of the aspect ratio L/w. All the results shown in this study have been, more specifically, calculated using the model of De La Torre et al. providing an effective numerical approximation of the $f\left(\frac{L}{w}\right)$ function for nanorods [8].

Anisotropic particles:

In order to evaluate the DDLS setup performances, three different suspensions of gold nanorods were analyzed by DDLS. Samples Au-NR1 and Au-NR2 were synthesized using a protocol derived from the “Turkevitch” method, well described in literature [9,10,11], and allowing an effective control of particles shape. In particular, this method implies the use of Cetyl Trimethylammonium Bromide (CTAB) surfactants which orient the particles growth towards anisotropic shape by blocking certain crystal facets growth. Multiple washing steps by centrifugation are performed to avoid the undesirable presence of CTAB micelles but note that CTAB remain at the surface of particles after their growth.

A first estimation of the size and aspect ratio of these NPs was achieved from Transmission Electron Microscopy (TEM) micrographs acquired with LVEM5 bench microscope operating at an acceleration voltage of 5 kV. The average dimensions of nanorods determined from these observations (100 particles count) are reported in the table 1. It should also be noted that DDLS considers the hydrodynamic dimension of particles which involves the layers of surfactant adsorbed to their surface as well as the solvation layer. To take surfactants into account when comparing TEM and DDLS results, the theoretical hydrodynamic sizes of Au-NR1 and Au-NR2 were estimated by considering a CTAB bilayer thickness of 3.2nm [12] and by adding value to the TEM measurements (see Table 1).

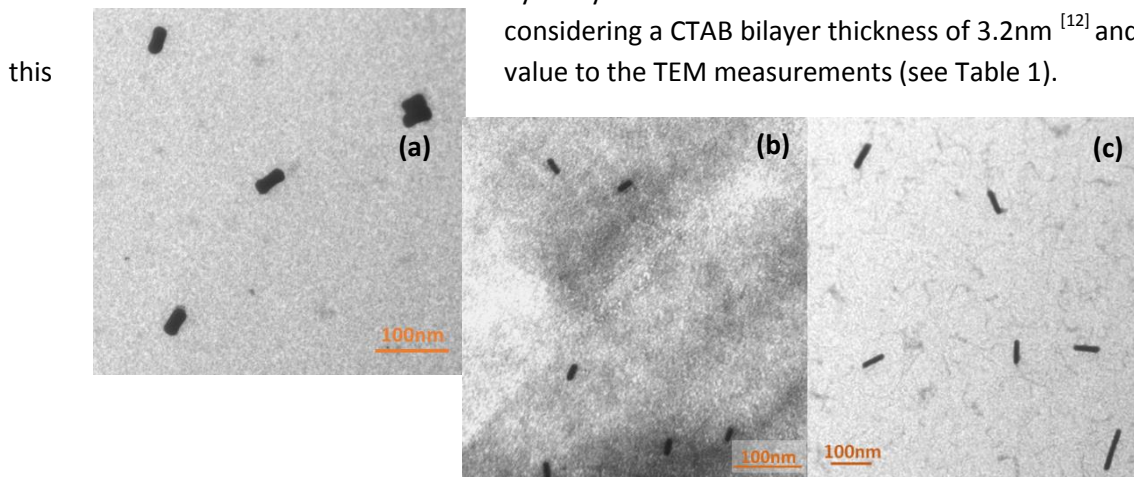


Figure 4: Electron micrographs of samples Au-NR1(a), Au-NR2(b) and Au-NR3(c).

Sample Au-NR3, is a commercial product purchased from the Company Nanocomposix (Product n° GRCN980 – lot n°ASP0002). The manufacturer provides the average sizes determined by TEM (JEOL 1010) also reported in table 1. These particles are stabilized using citrates and their hydrodynamic sizes

should be lower than CTAB bilayer. The average hydrodynamic diameter determined by the manufacturer using standard DLS is 6nm. This value obviously doesn't describe the nanorods correctly since it doesn't take into account their anisotropic properties.

		Au-NR1	Au-NR2	Au-NR3	
by	TEM sizes	L	41.5 ± 4.6nm	21.9 ± 2.3nm	59.9 ± 9.3nm
		w	19.8 ± 3.6nm	8.1 ± 1.0nm	10.1 ± 1.2nm
		L/w	2.1	2.7	6.0
only	Sizes with CTAB bilayer	L	47.9 ± 4.6nm	28.3 ± 2.3nm	
		w	26.2 ± 3.6nm	14.5 ± 1.0nm	
		L/w	1.8	1.9	

Table 1: Average dimensions of nanorods determined from TEM observations. In case of Au-NR1 and Au-NR2, is also reported the sizes considering the CTAB bilayer thickness.

DDLS measurements results:

Samples were analyzed by DDLS using the instrument Thetis®. In each case, measurements were performed by varying the scattering angle from 30 to 150°, acquiring both v-h and v-h data.

Figure 5 shows an example of corresponding ACFs obtained at 7 scattering angles for sample Au-NR1 and normalized, respectively v-v ACFs on figure 5(a) and v-h ACFs on figure 5(b). In particular, one can notice on figure 5(a) the angular dependency of the slow decay rate (corresponding to the $\exp[-\Gamma_t \cdot \tau]$ component of \mathbf{G}_w in eq 1). This illustrates the linear evolution of Γ_t upon q^2 (see eq.3). On the other hand, the fast decay rate (corresponding to the $\exp[-(\Gamma_r + \Gamma_t) \cdot \tau]$ mixed component of \mathbf{G}_w and \mathbf{G}_{vh} in eqs 1 and 2) shows a much lower change upon the angle of analysis. This behavior is explained by a quite higher value of Γ_r rate in comparison to Γ_t rate on the whole ϑ range and the fact that the rotational decay rate Γ_r is not q

dependent (see eq.4). As the ratio of D_r and D_t is inversely proportional to the length to the power 2 (see eqs 5 and 6), the shift of the v-h ACV curves with the scattering angle would be more visible for cylindrical NPs of much larger length.

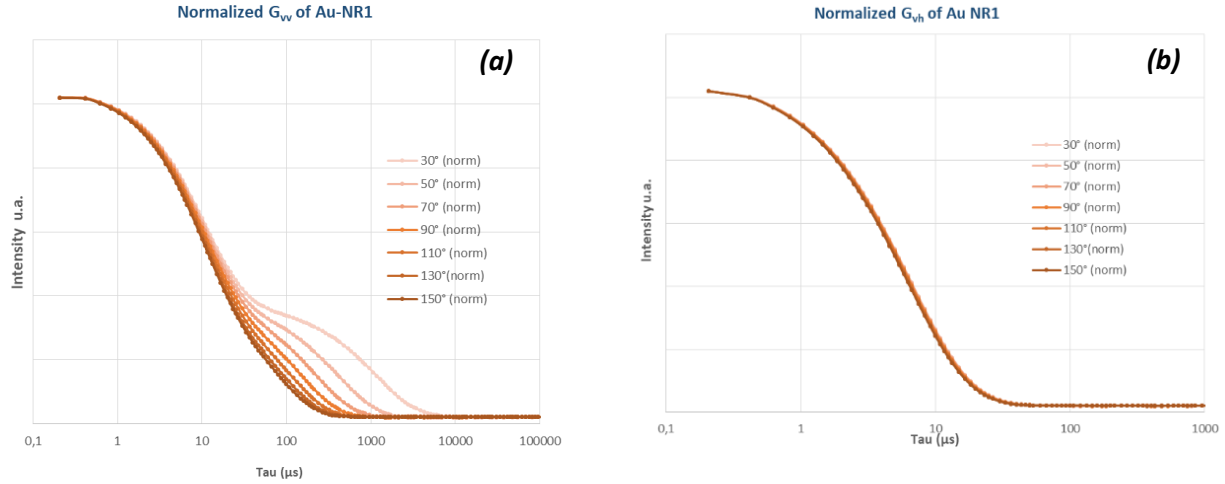


Figure 5: Autocorrelation functions measured for sample Au-NR1 at various scattering angles between 30 and 150°, from the respective scattered intensity fluctuations of (a) $I_{vv}(t)$ and (b) $I_{vh}(t)$.

Using the SBL multimodal algorithm, the ProTheta[®] software extracts the decay rate values from each ACF and plots them as a function of q^2 . Figure 6 illustrates the graph obtained by plotting the $(\Gamma_r + \Gamma_t)$ and Γ_t data of $G_{vv}(\tau)$ measurements for Au-NR1.

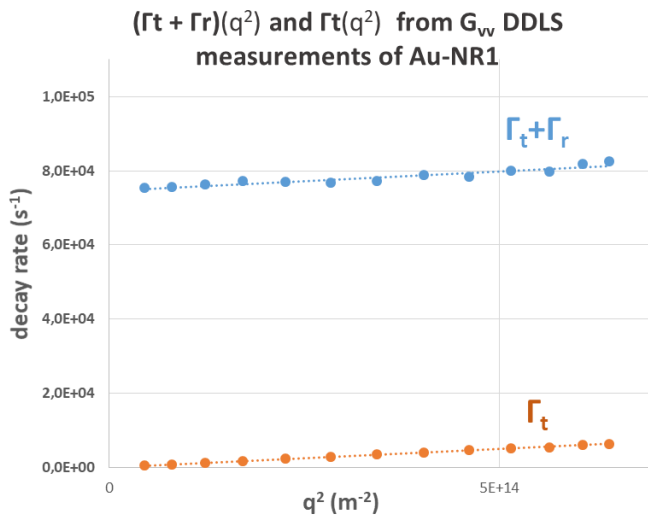


Figure 6: Decay rates determined by fitting the autocorrelation functions $G_{vv}(\tau)$ of Au-NR1 and plotted as a function of q^2 .

First, we checked that the decay rates measured for Au-NR1 well behaved as expected for anisotropic particles. In particular, we observed the linear and parallel trend of decay rates upon q^2 and the fact that $(\Gamma_r + \Gamma_t)(q^2)$ can be extrapolated to non-zero value when q tends towards 0, which is the signature of a rotational diffusion component. As described in the measurement principles, slope of the linear regressions allows us to determine a translational diffusion coefficient and the extrapolation of $(\Gamma_r + \Gamma_t)(q^2)$ at $q = 0$, a rotational diffusion coefficient. In this particular case, $D_t = 9.93 \cdot 10^6 \text{ nm}^2\text{s}^{-1}$ and $D_r = 1.24 \cdot 10^4 \text{ s}^{-1}$.

Finally, using the model of De La Torre et al. for cylindrical shapes^[8], hydrodynamic dimensions of Au-NR1 were calculated from these diffusion coefficients at $L = 46\text{nm}$ and $L/w = 1.38$ (and thus, $w = 34.8\text{nm}$).

The same method was applied on Au-NR2 and Au-NR3 and the corresponding results are reported in Table 2 below:

		Au-NR1	Au-NR2	Au-NR3
TEM sizes *+ CTAB bilayer thickness	L (nm)	47.9 *	28.3 *	59.9
	w (nm)	26.2 *	14.5 *	10.1
	L/w	1.8	1.9	6.0
DDLS measurement	D_t (nm ² .s ⁻¹)	9.93 10 ⁶	1.89 10 ⁷	1.37 10 ⁷
	D_r (s ⁻¹)	1.24 10 ⁴	7.19 10 ⁴	1.37 10 ⁴
	L (nm)	46.0	28.3	70.7
	w (nm)	34.8	16.9	14.2
	L/w	1.3	1.7	5.0

Table 2: Diffusion coefficients and sizes of nanorods determined from the DDLS measurements and TEM observations. In case of Au-NR1 and Au-NR2, the TEM sizes are reported considering the CTAB bilayer thickness.

Discussion:

Table 2 shows that the size measurements obtained by DDLS are globally very consistent with what is expected from the TEM observations, thereby highlighting the relevance and robustness of the method. In particular, we demonstrated that both the length and the aspect ratio of small Au-NR2 nanorods can be accurately determined with Thetis[®] DDLS setup. However, two values deviate significantly from the TEM results: the aspect ratio of Au-NR1 measured by DDLS as 1.3 instead of 1.8, which brings to the calculation of a larger rod hydrodynamic diameter and the length of Au-NR3, which is 18% higher than the average TEM size. In the case of Au-NR1 particles, it seems that their shape irregularity could be some of the main reasons behind this result. Actually, TEM micrographs shows that these rods are not perfectly cylindrical and with a more rounded shape for some of them. This could induce to an underestimation of the corresponding overall aspect ratios. One can also note that with a L/w value of 1.7, the expected aspect ratio is theoretically below the limit of validity of the used hydrodynamic model (defined for $L/w \geq 2$)^[8], which can obviously cause some deviation of the experiment from the model description. In case of Au-NR3, we ascribe the longer dimension to the polydispersity in length of these commercial rods. Actually, the standard deviation of length measured by the manufacturer with TEM is 9.3nm (1.2nm for the diameter). Yet, the average results in DDLS (like in DLS) are weighted in scattered light intensity while they are weighted in number of particles by TEM counting method. Since larger particles scattered much more light intensity than smaller one, light scattering measurement shifts dimensions to larger sizes especially as the width of size distribution is large. Finally, the impact of the solvation layer has not been taken into account for Au-NR3 and it is well know that it generally makes the hydrodynamic sizes of dense particles several nanometers larger than the TEM core sizes.

Conclusion:

The use of DDLS technique in a first industrial instrument presents a unique and real advantage for the development of new advanced materials. We have shown here that results obtained for specific anisotropic nanoparticles are consistent with TEM measurements. DDLS is now mature enough to be used at a large scale for all specific application using anisotropic nanoparticles. One can even see Thetis as a multiangle DLS and DDLS tool for all nanoparticle characterization.

Acknowledgements:

We would like to thank Olivier Sandre and Florian Aubrit, from LCPO CNRS/University and INP Bordeaux, with whom this fruitful work has been carried out.

References:

- [1] Reddy N.K. et al «Flow Dichroism as a Reliable Method To Measure the Hydrodynamic Aspect Ratio of Gold Nanoparticles», ACS Nano., 2011, V. 5. № 6, 4935–4944
- [2] Sacanna S.; Pine D. J. “Shape-anisotropic colloids: Building blocks for complex assemblies” Current Opinion in Colloid & Interface Science, 2011, V. 16 (2), 96-105
- [3] Turner, Leaf (1973). "Rayleigh-Gans-Born Light Scattering by Ensembles of Randomly Oriented Anisotropic Particles". Applied Optics. 12 (5): 1085–1090
- [4] F. Aubrit, D. Jacob, O. Sandre, “Device and method for determining characteristic parameters of the dimensions of nanoparticles”, Applicants: Cordouan Technologies, CNRS, Univ. Bordeaux, IPB. FR3100333 B1 (2021/09/17), EP3789750 A1 (2021/3/10), US11156540 B2 (2021/10/26). Priority date: 2019/09/03. <https://www.cordouan-tech.com/thetis/>
- [5] Berne, B. J.; Pecora, R. Dynamic Light Scattering: WileyInterscience: New York, 1976.
- [6] Zero, K.; Pecora, R. In Dynamic Light Scattering; Pecora, R., Ed.; Plenum Press: New York, 1985; p59
- [7] Eimer W., Pecora R. J. Chem. Phys. 1991, 94, 2324-2329
- [8] Garcia de la Torre, M. C. Lopez Martinez, and M. hl. Tirado, Biopolymers 23, 611 (1984).
- [9] Turkevitch. Colloidal Gold. part I. Gold Bulletin, 18:86–91, 1985.
- [10] Sau T K and Murphy C. J., Langmuir 20, 6414-6420 (2004).
- [11] Scarabelli, A. Sánchez-Iglesias, J. Rérez-Juste, and L. M. Liz-Mán. A “Tips and Tricks” Practical Guide to the Synthesis of Gold Nanorods. Journal of Chemistry Letters, 6:4270–4279, 2015
- [12] Sergio Gómez-Graña 1 , Fabien Hubert, Fabienne Testard, Andrés Guerrero-Martínez, Isabelle Grillo, Luis M Liz-Marzán, Olivier Spalla Surfactant (bi)layers on gold nanorods, Langmuir. 2012 Jan 17;28(2):1453-9